Engineering Notes

Equations of Motion of Rotary-Wing Unmanned Aerial System with Time-Varying Inertial Properties

Andrea L'Afflitto* and Keyvan Mohammadi†
The University of Oklahoma, Norman, Oklahoma 73019

DOI: 10.2514/1.G003015

Nomenclature

F	=	external forces acting on $\mathcal{V}$
I	=	matrix of inertia of the unmanned aerial system and its payload
$\mathbb{I}$	=	inertial reference frame centered in O
$\mathbb{J}$	=	unmanned aerial system reference frame centered in A
M	=	moment of the external forces
M_T	=	moment of the force due to mass variation
m	=	mass of the unmanned aerial system and its payload
$\mathcal{P}_i$	=	volume containing the ith propeller
r_A	=	position of A from O
r_C	=	position of the center of mass C with respect to A
r_{mA}	=	position of the infinitesimal mass δm with respect to A
r_{mC}	=	position of δm with respect to C
T	=	force due to mass variation
$\mathcal{V}$	=	volume containing both the unmanned aerial system and its payload
v_A	=	velocity of A with respect to $\mathbb{I}$
$[\phi, \theta, \psi]$	=	angular position of $\mathbb{I}$ with respect to $\mathbb{J}$
Ω_{P_i}	=	angular rate of the ith propeller
ω	=	angular velocity of $\mathbb{I}$ with respect to $\mathbb{J}$

I. Introduction

ROTARY-WING unmanned aerial systems (UASs), such as quadrotors, hexrotors, and octorotors, have drawn considerable attention in the past decade [1], ([2] pp. 2–7), [3,4]. Thus far, these platforms have been mostly used for remote sensing applications, such as surveying some geographic areas, monitoring crops, and inspecting infrastructures. One of the next frontiers for rotary-wing UASs is to perform tasks that require direct interaction with the environment, such as manipulating and transporting objects [5–9] for which the inertial properties are unknown. Significant limitations to the use of UASs for these applications are the low capacity of energy storage systems and the need for reliable control systems that allow completing the mission objectives in spite of errors in the UAS model, unknown reaction forces, and uncertainties introduced by the payload. For instance, the UAS mass, center of mass, and inertia matrix may vary substantially by uplifting and deploying some payload of unknown inertial properties. Moreover, if the payload is connected to the UAS through flexible structures, such as ropes, these variations are more significant; and the UAS control system must be robust to these changes [10]. Similarly, to extend the endurance of UASs beyond the current capabilities of electric batteries, a solution is to employ fuel cells and fuel-based motors [11]. In this case, the UAS mass is a decreasing function of time, and the effect of fluid fuel sloshing must be accounted for in the dynamical model and compensated by the control system.

Numerous researchers are involved in the design and implementation of robust control design techniques for UASs, ranging from the classical $\mathcal{H}_\infty$ control [12] and the linear-quadratic Gaussian [13] control to more advanced ones, such as the robust feedback linearization [14], the model reference adaptive control [15,16], and the sliding-mode control [17]. Having accurate models of the UAS dynamics, control engineers can make less conservative assumptions on the closed-loop system's uncertainties and design efficient robust controllers.

The equations of motion of rotary-wing UASs can be deduced using the Newton–Euler approach or the Euler–Lagrange approach. All publications found by the authors, where the equations of motion of rotary-wing UASs were derived, assumed that the UAS mass was constant and the position of the vehicle's center of mass was known ([2] p. 28), [18–20]. Some proofs based on the Newton–Euler approach accounted for the gyroscopic effect only and neglected the inertial countertorque. Some proofs accounted for both the inertial countertorque and the gyroscopic effect as external moments of the forces, but this approach is not formally justifiable. The proofs based on the Euler–Lagrange approach, such as those in ([2] pp. 25–28) and ([21] pp. 99–102), involved trigonometric polynomials in the Coriolis term, and hence the computational complexity of the control laws designed using this characterization of the rotational dynamics is high.

In this engineering Note, we apply the Newton–Euler approach and deduce in a tutorial manner the equations of motion of rotary-wing UASs, for which the inertial properties, such as the mass and matrix of inertia, are not constant in time. Moreover, in our approach, the UAS reference frame is centered in a point that does not necessarily coincide with the UAS center of mass. Thus, our framework is suitable for control problems, wherein the location of the vehicle's center of mass is unknown and not fixed in the UAS. The unforced dynamic equations presented in this Note involve polynomial nonlinearities only, and it is worthwhile recalling that the polynomial evaluation has complexity $O(n)$ [22], which is generally considered as low. Lastly, by assuming that the UAS mass is constant, the center of mass is known, the payload is rigidly connected to the UAS, and both the UAS frame and the propellers are rigid bodies, we deduce the equations of motion of rotary-wing UASs that are commonly available in the literature. A numerical example illustrates the applicability of the theoretical results exposed herein.

II. Notation

In this Note, we denote by N the number of propellers of a UAS; $\mathbb{I}$ as an orthonormal inertial reference frame centered in O; $\mathcal{V} \subset \mathbb{R}^3$ as a volume containing the UAS and its payload; $\mathbb{J}$ as an orthonormal reference frame fixed with the UAS and centered in a point $A \in \mathcal{V}$; and $\mathcal{P}_i \subset \mathbb{R}^3$, $i = 1, \ldots, N$, as a volume exclusively containing the ith propeller (see Fig. 1). If a vector $a \in \mathbb{R}^3$ is expressed in the reference frame $\mathbb{I}$, then it is denoted by $a^{\mathbb{I}}$; if a vector is expressed in $\mathbb{J}$, then no superscript is used. Given $a = [a_1, a_2, a_3]^{\mathrm{T}} \in \mathbb{R}^3$

Received 3 May 2017; revision received 2 July 2017; accepted for publication 5 July 2017; published online 25 August 2017.

*Assistant Professor, School of Aerospace and Mechanical Engineering; a.lafflitto@ou.edu. Senior Member AIAA.

†Graduate Research Assistant, School of Aerospace and Mechanical Engineering; keyvan.mohammadi@ou.edu.

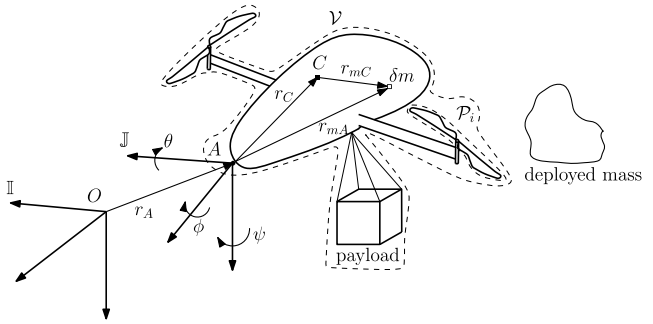

Fig. 1 Model of a UAS and its payload, which is not rigidly attached.

$$a^{\times} \triangleq \begin{bmatrix} 0 & -a_3 & a_2 \\ a_3 & 0 & -a_1 \\ -a_2 & a_1 & 0 \end{bmatrix}$$

denotes the cross-product operator.

The position of the reference point A with respect to the origin O of the reference frame $\mathbb{I}$ is denoted by $r_A{:}[0,\infty) \to \mathbb{R}^3$, the velocity of A with respect to $\mathbb{I}$ is denoted by $v_A{:}[0,\infty) \to \mathbb{R}^3$, and the position of the UAS center of mass C with respect to the reference point A is denoted by $r_C{:}[0,\infty) \to \mathcal{V}$. Let $r_{mA}{:}[0,\infty) \to \mathcal{V}$ denote the position of a generic point in $\mathcal{V}$ with respect to A and $\delta m{:}[0,\infty) \to \mathbb{R}$ the mass of an infinitesimal volume centered in $r_{mA}(\cdot)$. We denote by $r_{mO}{:}[0,\infty) \to \mathcal{V}$ the position of the center of this infinitesimal volume with respect to O, and we denote $r_{mC}{:}[0,\infty) \to \mathcal{V}$ as the position of the center of this infinitesimal volume from C; see Fig. 1. The sum of the external forces acting on $\delta m(\cdot)$ is denoted by $\delta F{:}[0,\infty) \to \mathbb{R}^3$. Part of the arbitrarily small mass $\delta m(t)$, $t \geq 0$, may be deployed from the UAS at some time $t_2 \geq t$ with nonzero velocity; we denote by $u{:}[0,\infty) \to \mathcal{V}$ the exhaust velocity: that is, the velocity of the part of the mass $\delta m(\cdot)$ that is expelled from the volume $\mathcal{V}$.

In this Note, we denote by $\phi, \psi{:}[0,\infty) \to [0, 2\pi)$ the roll and yaw angles, respectively;

$$\theta{:}[0,\infty) \to \left(-\frac{\pi}{2}, \frac{\pi}{2}\right)$$

as the pitch angle; $\omega{:}[0,\infty) \to \mathbb{R}^3$ as the angular velocity of $\mathbb{J}$ with respect to $\mathbb{I}$; and $\omega_{P_i}{:}[0,\infty) \to \mathbb{R}^3$ as the angular velocity of the ith propeller, $i = 1, \ldots, N$, with respect to $\mathbb{J}$ (see Fig. 1).

III. Kinematics and Dynamics of a Variable-Mass UAS

The kinematic equations of a UAS capture the motion of the reference frame $\mathbb{J}$ with respect to the reference frame $\mathbb{I}$ and do not depend on the modeling assumptions on the UAS. Specifically, the translational kinematic equation of a UAS is given by ([23] example 1.12)

$$\dot{r}_A^{\mathbb{I}}(t) = \begin{bmatrix} \cos\psi(t) & -\sin\psi(t) & 0 \\ \sin\psi(t) & \cos\psi(t) & 0 \\ 0 & 0 & 1 \end{bmatrix} \begin{bmatrix} \cos\theta(t) & 0 & \sin\theta(t) \\ 0 & 1 & 0 \\ -\sin\theta(t) & 0 & \cos\theta(t) \end{bmatrix} \cdot \begin{bmatrix} 1 & 0 & 0 \\ 0 & \cos\phi(t) & -\sin\phi(t) \\ 0 & \sin\phi(t) & \cos\phi(t) \end{bmatrix} v_A(t),$$
$$r_A^{\mathbb{I}}(0) = r_{A,0}^{\mathbb{I}}, \qquad t \geq 0 \quad (1)$$

and the rotational kinematic equation of a UAS is given by ([23] theorem 1.7)

$$\begin{bmatrix} \dot{\phi}(t) \\ \dot{\theta}(t) \\ \dot{\psi}(t) \end{bmatrix} = \begin{bmatrix} 1 & \sin\phi(t)\tan\theta(t) & \cos\phi(t)\tan\theta(t) \\ 0 & \cos\phi(t) & -\sin\phi(t) \\ 0 & \sin\phi(t)\sec\theta(t) & \cos\phi(t)\sec\theta(t) \end{bmatrix} \omega(t),$$
$$\begin{bmatrix} \phi(0) \\ \theta(0) \\ \psi(0) \end{bmatrix} = \begin{bmatrix} \phi_0 \\ \theta_0 \\ \psi_0 \end{bmatrix} \quad (2)$$

Equation (1) relates the translational velocity of point A with respect to $\mathbb{I}$, which is expressed in the reference frame $\mathbb{J}$, to the time derivative of the translational position of A in the inertial reference frame $\mathbb{I}$. Equation (2) relates the angular velocity of $\mathbb{J}$ with respect to $\mathbb{I}$, which per definition is expressed in the reference frame $\mathbb{J}$ ([23] definition 1.9), with the time derivative of the angular position of the reference frame $\mathbb{J}$ with respect to $\mathbb{I}$.

To capture the dynamics of variable-mass rotary-wing UASs, we apply Newton's law to each infinitesimal mass $\delta m(\cdot)$ contained in $\mathcal{V}$. Specifically, let $\delta m(t)\dot{r}_{mO}^{\mathbb{I}}(t)$ denote the momentum of $\delta m(\cdot)$ at the time instant $t \geq 0$. In the first approximation, the momentum of the same infinitesimal mass at $t_2 \geq t \geq 0$ is given by

$$[\delta m(t_2) + \delta\dot{m}(t_2)(t_2 - t)][\dot{r}_{mO}^{\mathbb{I}}(t_2) + \ddot{r}_{mO}^{\mathbb{I}}(t_2)(t - t_2)] - \delta\dot{m}(t_2)[\dot{r}_{mO}^{\mathbb{I}}(t_2) + u^{\mathbb{I}}(t_2)](t_2 - t) \quad (3)$$

The term

$$[\delta m(t_2) + \delta\dot{m}(t_2)(t_2 - t)][\dot{r}_{mO}^{\mathbb{I}}(t_2) + \ddot{r}_{mO}^{\mathbb{I}}(t_2)(t - t_2)]$$

$t_2 \geq t \geq 0$, captures the momentum of the part of the infinitesimal mass that remains in the UAS at t_2, and the term $-\delta\dot{m}(t_2)[\dot{r}_{mO}^{\mathbb{I}}(t_2) + u^{\mathbb{I}}(t_2)](t_2 - t)$ captures the momentum of the part of the infinitesimal mass that is leaving the UAS at the time instant t_2 with exhaust velocity $u^{\mathbb{I}}(t_2)$. Thus, it follows from Newton's law [24] that

$$\delta F^{\mathbb{I}}(t) = \lim_{t_2 \to t^+} \frac{[\delta m(t_2) + \delta\dot{m}(t_2)(t_2 - t)][\dot{r}_{mO}^{\mathbb{I}}(t_2) + \ddot{r}_{mO}^{\mathbb{I}}(t_2)(t - t_2)]}{t_2 - t} - \lim_{t_2 \to t^+} \frac{\delta\dot{m}(t_2)[\dot{r}_{mO}^{\mathbb{I}}(t_2) + u^{\mathbb{I}}(t_2)](t_2 - t) + \delta m(t)\dot{r}_{mO}^{\mathbb{I}}(t)}{t_2 - t}$$
$$= \delta m(t)\ddot{r}_{mO}^{\mathbb{I}}(t) - \delta\dot{m}(t)u^{\mathbb{I}}(t), \qquad r_{mO}^{\mathbb{I}}(0) = r_{mO,0}^{\mathbb{I}}, \quad \dot{r}_{mO}^{\mathbb{I}}(0) = v_{mO,0}^{\mathbb{I}}, \qquad t \geq 0 \quad (4)$$

Because $r_{mO}^{\mathbb{I}}(t) = r_A^{\mathbb{I}}(t) + r_C^{\mathbb{I}}(t) + r_{mC}^{\mathbb{I}}(t)$, $t \geq 0$, Eq. (4) is equivalent to

$$\delta F^{\mathbb{I}}(t) + \delta\dot{m}(t)u^{\mathbb{I}}(t) = \delta m(t)[\dot{v}_A^{\mathbb{I}}(t) + \ddot{r}_C^{\mathbb{I}}(t) + \ddot{r}_{mC}^{\mathbb{I}}(t)], \qquad r_{mO}^{\mathbb{I}}(0) = r_{mO,0}^{\mathbb{I}}, \quad \dot{r}_{mO}^{\mathbb{I}}(0) = v_{mO,0}^{\mathbb{I}}, \qquad t \geq 0 \quad (5)$$

It is common practice in aeronautical engineering to express vectors in the reference frame $\mathbb{J}$ attached to the UAS. To express Eq. (5) in the reference frame $\mathbb{J}$, we recall that, by theorem 1.3 of [23],

$$\dot{v}_A^{\mathbb{I}}(t) = \dot{v}_A(t) + \omega^{\times}(t)v_A(t), \qquad t \geq 0 \quad (6)$$

and, by example 1.4 of [23],

$$\ddot{r}_C^{\mathbb{I}}(t) = \ddot{r}_C(t) + \dot{\omega}^{\times}(t)r_C(t) + 2\omega^{\times}(t)\dot{r}_C(t) + \omega^{\times}(t)\omega^{\times}(t)r_C(t) \quad (7)$$

It follows from the definition of the center of mass ([23] definition 1.30) that $\int_{\mathcal{V}} r_{mC}(t)\delta m(t) = 0$ $t \geq 0$; hence, it follows from Eqs. (5–7) that the translational dynamic equation of a variable-mass rotary-wing UAS is given by

$$F(t) + T(t) = m(t)[\dot{v}_A(t) + \omega^\times(t)v_A(t) + \ddot{r}_C(t) + \dot{\omega}^\times(t)r_C(t) + 2\omega^\times(t)\dot{r}_C(t) + \omega^\times(t)\omega^\times(t)r_C(t)], \quad v_A(0) = v_{A,0}, \quad t \geq 0 \quad (8)$$

where

$$F(t) \triangleq \int_{\mathcal{V}} \delta F(t)$$

denotes the sum of the external forces acting on $\mathcal{V}$, including the force produced by the propellers;

$$m(t) = \int_{\mathcal{V}} \delta m(t)$$

denotes the UAS and payload's mass; and

$$T(t) \triangleq \int_{\mathcal{V}} u(t)\delta\dot{m}(t)$$

Equation (8) is expressed in the reference frame $\mathbb{J}$. Note that the right-hand side of Eq. (8) is not an explicit function of the propellers' angular velocities. The term $T(t)$, $t \geq 0$, denotes the force generated according to Newton's third law for deploying some mass from the control volume $\mathcal{V}$. In practice, $r_C(\cdot)$ is not precisely known; hence, the terms in Eq. (8) involving $r_C(\cdot)$ should be considered as uncertain.

Forces acting on UASs are typically the gravity ([23] example 2.3):

$$F_g(t, \phi, \theta) = m(t)g[-\sin\theta, \cos\theta\sin\phi, \cos\theta\cos\phi]^T, \quad (t, \phi, \theta) \in [0, \infty) \times [0, 2\pi) \times \left(-\frac{\pi}{2}, \frac{\pi}{2}\right) \quad (9)$$

where g denotes the gravitational acceleration, the aerodynamic forces induced by the motion of the UAS with respect to the wind, and the aerodynamic forces induced by the propellers [19]. In publications concerning rotary-wing UASs, the component of each propeller's force perpendicular to the rotor's disk is referred to as the thrust force. It is important to note that $T(\cdot)$ in Eq. (8) is not produced by the UAS propellers, but it is generated by the deployment of some mass from the UAS.

It follows from Eq. (4) that

$$\int_{\mathcal{V}} [r^{\mathbb{I}}_{mA}(t)]^\times [\ddot{r}^{\mathbb{I}}_{mO}(t)\delta m(t) - u^{\mathbb{I}}(t)\delta\dot{m}(t) - \delta F^{\mathbb{I}}(t)] = 0$$

$t \geq 0$. Therefore, because $r_{mA}(t) = r_C(t) + r_{mC}(t)$, $t \geq 0$, and $r_{mO}(t) = r_A(t) + r_{mA}(t)$, it holds that

$$M^{\mathbb{I}}(t) + M^{\mathbb{I}}_T(t) = \int_{\mathcal{V}} [r^{\mathbb{I}}_C(t) + r^{\mathbb{I}}_{mC}(t)]^\times \dot{v}^{\mathbb{I}}_A(t)\delta m(t) + \int_{\mathcal{V}} [r^{\mathbb{I}}_{mA}(t)]^\times \ddot{r}^{\mathbb{I}}_{mA}(t)\delta m(t)$$

where

$$M(t) \triangleq \int_{\mathcal{V}} r^\times_{mA}(t)\delta F(t)$$

and

$$M_T(t) \triangleq \int_{\mathcal{V}} r^\times_{mA}(t)u(t)\delta\dot{m}(t)$$

denote the moment of the external forces and the moment of the force $T(\cdot)$ with respect to A, respectively; and it follows from the definition of the center of mass Eq. (6), and example 1.4 of [23] that

$$M(t) + M_T(t) = m(t)r^\times_C(t)[\dot{v}_A(t) + \omega^\times(t)v_A(t)] + \int_{\mathcal{V}} r^\times_{mA}(t)[\dot{\omega}^\times(t)r_{mA}(t)]\delta m(t) + \int_{\mathcal{V}} r^\times_{mA}(t)[\omega^\times(t)\omega^\times(t)r_{mA}(t) + \ddot{r}_{mA}(t) + 2\omega^\times(t)\dot{r}_{mA}(t)]\delta m(t), \quad t \geq 0 \quad (10)$$

It holds that

$$r^\times_{mA}(t)\omega^\times(t)\omega^\times(t)r_{mA}(t) = -\omega^\times(t)r^\times_{mA}(t)r^\times_{mA}(t)\omega(t)$$

$t \geq 0$, and it follows from the Jacobi identity ([23] example 1.7) that

$$r^\times_{mA}(t)\omega^\times(t)\dot{r}_{mA}(t) = \omega^\times(t)r^\times_{mA}(t)\dot{r}_{mA}(t) + \dot{r}^\times_{mA}(t)\omega^\times(t)r_{mA}(t)$$

Hence, it follows from Eq. (10) that the rotational dynamic equation of a variable-mass rotary-wing UAS is given by

$$M(t) + M_T(t) = m(t)r^\times_C(t)[\dot{v}_A(t) + \omega^\times(t)v_A(t)] + I(t)\dot{\omega}(t) + \omega^\times(t)I(t)\omega(t) + \dot{h}(t) + \omega^\times(t)h(t) + J(t)\omega(t) + \dot{I}(t)\omega(t), \quad \omega(0) = \omega_0, \quad t \geq 0 \quad (11)$$

where

$$I(t) \triangleq -\int_{\mathcal{V}} r^\times_{mA}(t)r^\times_{mA}(t)\delta m(t)$$

$$J(t) \triangleq \int_{\mathcal{V}} r^\times_{mA}(t)r^\times_{mA}(t)\delta\dot{m}(t)$$

and

$$h(t) \triangleq \int_{\mathcal{V}} r^\times_{mA}(t)\dot{r}_{mA}(t)\delta m(t)$$

Equation (11) is expressed in the reference frame $\mathbb{J}$. The term $I(t)$, $t \geq 0$, denotes the inertia matrix of the UAS and its payload with respect to the reference point A; the term $J(t)$ captures the variation in the UAS moment of inertia due to the variation of the vehicle's mass over time; $h(t)$ captures the contribution of moving components, such as the propellers, to the quadrotor's angular momentum; and $M_T(t)$ denotes the moment of the force generated by deploying some mass from the control volume $\mathcal{V}$. If $r_{mA}(t)$, $t \geq 0$, denotes the position of an infinitesimal volume of mass $\delta m(t)$ located on one of the propellers, then it follows from theorem 1.2 of [23] that the propellers' angular velocities affect $\dot{r}_{mA}(t)$. Thus, although the propellers' angular velocities do not appear explicitly in the right-hand side of Eq. (11), these directly affect $h(t)$ $\dot{h}(t)$, and $\dot{I}(t)$. Because $\dot{r}_{mA}(t)$, $t \geq 0$, does not appear in the definition of $J(t)$, the propellers' angular velocities do not directly affect $J(t)$.

IV. Dynamic Equations of Rotary-Wing UAS with Constant Inertial Properties

In this section, we specialize the results proven in Sec. III and deduce the classical dynamic equations of rotary-wing UAS assuming that the UAS mass is constant, both the UAS frame and the propellers are rigid bodies, and the position of the UAS center of mass is known. Specifically, if the UAS and payload's mass $m(\cdot)$ are constant, then $T(t) = 0$, $t \geq 0$, $M_T(t) = 0$, and $J(t) = 0$. Moreover, if the center of mass C can be identified, then it is convenient to choose $A \equiv C$, which implies that $r_C(t) = 0$, $t \geq 0$. Therefore, in this case, Eq. (8) is equivalent to

$$F(t) = m[\dot{v}_A(t) + \omega^\times(t)v_A(t)], \quad v_A(0) = v_{A,0}, \quad t \geq 0 \quad (12)$$

which is commonly used in the literature to capture the translational dynamics of rotary-wing UASs [25].

Assuming that the payload is rigidly connected to the UAS and modeling both the UAS frame and the propellers as rigid bodies, it holds that

$$\int_{\mathcal{V}[\cup_i^N \mathcal{P}_i]} r_{mA}^{\times}(t)\dot{r}_{mA}(t)\delta m = 0$$

$t \geq 0$, and it follows from theorem 1.2 of [23] that

$$h(t) = \sum_{i=1}^{N} \int_{\mathcal{P}_i} r_{mA}^{\times}(t)\omega_{P_i}^{\times}(t) r_{mA}(t)\delta m$$

and

$$\dot{h}(t) = \sum_{i=1}^{N} \int_{\mathcal{P}_i} r_{mA}^{\times}(t)[\dot{\omega}_{P_i}^{\times}(t) r_{mA}(t) + \omega_{P_i}^{\times}(t)\omega_{P_i}^{\times}(t) r_{mA}(t)]\delta m$$

Thus, Eq. (11) reduces to

$$\begin{aligned} M(t) &= I(t)\dot{\omega}(t) + \omega^{\times}(t)I(t)\omega(t) \\ &\quad + \sum_{i=1}^{N}[I_{P_i}\dot{\omega}_{P_i}(t) + \omega_{P_i}^{\times}(t)I_{P_i}\omega_{P_i}(t)] \\ &\quad + \omega^{\times}(t)\sum_{i=1}^{N} I_{P_i}\omega_{P_i}(t) + \dot{I}(t)\omega(t), \\ &\qquad \omega(0) = \omega_0, \qquad t \geq 0 \end{aligned} \tag{13}$$

where

$$I_{P_i} \triangleq -\int_{\mathcal{P}_i} r_{mA}^{\times} r_{mA}^{\times}\delta m$$

denotes the matrix of inertia of the ith propeller, $i = 1, \ldots, N$, with respect to the reference point A. It is common practice to model propellers as thin disks, for which the angular velocity is given by $\omega_{P_i}(t) = [0, 0, \Omega_{P_i}(t)]^T$, $t \geq 0$, $i = 1, \ldots, N$. In this case, the inertia matrix I_{P_i}, $i = 1, \ldots, N$, is diagonal and $\omega_{P_i}^{\times}(t)I_{P_i}\omega_{P_i}(t) = 0$, $t \geq 0$. Moreover,

$$\dot{I}(t) = -\sum_{i=1}^{N}\int_{\mathcal{P}_i} \dot{r}_{mA}^{\times}(t) r_{mA}^{\times}(t)\delta m - \sum_{i=1}^{N}\int_{\mathcal{P}_i} r_{mA}^{\times}(t)\dot{r}_{mA}^{\times}(t)\delta m$$

$t \geq 0$, and because

$$\int_0^{2\pi} (\cos^2\tau - \sin^2\tau)\,\mathrm{d}\tau = 0$$

and

$$\int_0^{2\pi} \sin\tau\cos\tau\,\mathrm{d}\tau = 0$$

it can be proven that, in this case, $\dot{I}(t) = 0$, $t \geq 0$. Thus, it follows from Eq. (13) that the rotational equation of a constant-mass rotary-wing UAS, for which the position of the center of mass is known, for which the frame is modeled as a rigid body, for which the payload is rigidly attached to the frame, and for which the propellers are modeled as spinning disks, is given by

$$\begin{aligned} M(t) &= I\dot{\omega}(t) + \omega^{\times}(t)I\omega(t) + \sum_{i=1}^{N} I_{P_i}\begin{bmatrix} 0 \\ 0 \\ \dot{\Omega}_{P_i}(t) \end{bmatrix} \\ &\quad + \omega^{\times}(t)\sum_{i=1}^{N} I_{P_i}\begin{bmatrix} 0 \\ 0 \\ \Omega_{P_i}(t) \end{bmatrix}, \qquad \omega(0) = \omega_0, \qquad t \geq 0 \end{aligned} \tag{14}$$

The terms

$$\sum_{i=1}^{N} I_{P_i}[0, 0, \dot{\Omega}_{P_i}(t)]^T$$

$t \geq 0$, and

$$\omega^{\times}(t)\sum_{i=1}^{N} I_{P_i}[0, 0, \Omega_{P_i}(t)]^T$$

are known as the inertial countertorque and gyroscopic effect, respectively. Equation (14) is commonly used to capture the rotational dynamics of rotary-wing UASs [13].

V. Illustrative Numerical Example

In this section, we present a numerical example to illustrate the theoretical results of Sec. III. Specifically, we analyze the dynamics of a quadrotor helicopter of constant mass m_q, for which the frame is modeled as a rigid body and for which the propellers are modeled as thin disks. The quadrotor carries a reservoir modeled as a ball of unit radius and variable mass m_p:$[0, \infty) \to \mathbb{R}$, which is connected to one of the vehicle's arms at a distance $l \geq 0$ from the reference point A, which is located at the intersection of the quadrotor's arms. The orthonormal reference frame $\mathbb{J} = \{A; x(\cdot), y(\cdot), z(\cdot)\}$ is oriented so that the $z(\cdot)$ axis points downward and the $y(\cdot)$ axis is along one of the propellers' arms and points toward the reservoir for $l > 0$; see Fig. 2.

Three mission scenarios are considered. First, we assume that $m_p(t) = m_q$, $t \geq 0$, $l = 0$, and the reservoir is rigidly attached to the quadrotor. In the second scenario, the reservoir is connected to the quadrotor by a spring of stiffnesses $k > 0$ and $l > 0$; part of the reservoir's content is released over time with constant exhaust velocity $u(t) = u_{\text{exhaust},1}$, $t \in [0, t_2]$, so that $m_p(0) = 2.5m_q$, $m_p(t_2) = m_q$, and $\dot{m}_p(\cdot)$ is linear on $[0, t_2]$; at $t = t_2$, the spring is instantaneously removed and the reservoir is dropped. In the third scenario, $k > 0$, $l > 0$, $m_p(0) = 2.5m_q$, $m_p(t_2) = m_q$, $\dot{m}_p(\cdot)$ is linear on $[0, t_2]$, the reservoir's content is released with constant exhaust velocity $u(t) = u_{\text{exhaust},2}$, $t \in [0, t_2]$, but the reservoir is not dropped; that is, $m_p(t) = m_q$ and $u(t) = 0$ for all $t \geq t_2$.

We model the force $F(\cdot)$ as

$$F(t) = F_T(f_1(t)) + F_g(t, \phi(t), \theta(t)), \qquad t \geq 0 \tag{15}$$

where $F_T(f_1) = [0, 0, f_1]^T$, $f_1 \in \mathbb{R}$, and $F_g(t, \phi, \theta)$ is given by Eq. (9) with $m(t) = m_q + m_p(t)$. The control input $f_1(\cdot)$ is designed using a proportional-derivative feedback control law so that the quadrotor is able to hover in the first mission scenario. For simplicity, the aerodynamic forces are neglected and $M(t) = 0$, $t \geq 0$.

Consider a quadrotor of mass $m_q = 2$ kg, for which the propellers' radius is 0.1 m and for which the inertia matrix with respect to A, without payload and propellers, is given by

$$I_q = \begin{bmatrix} 1 & 0 & 0 \\ 0 & 1 & 0 \\ 0 & 0 & 1.2 \end{bmatrix} \text{ kg/m}^2$$

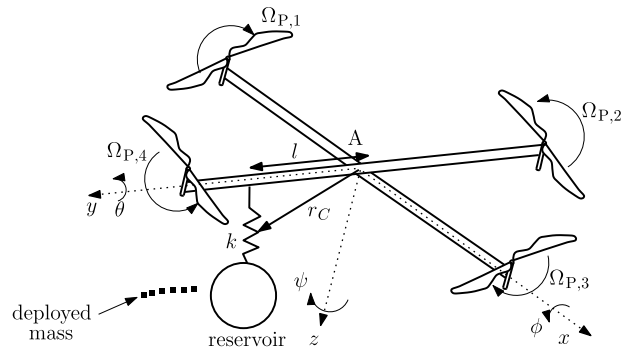

Fig. 2 Quadrotor helicopter with variable mass payload, which is connected to the aircraft by a spring.

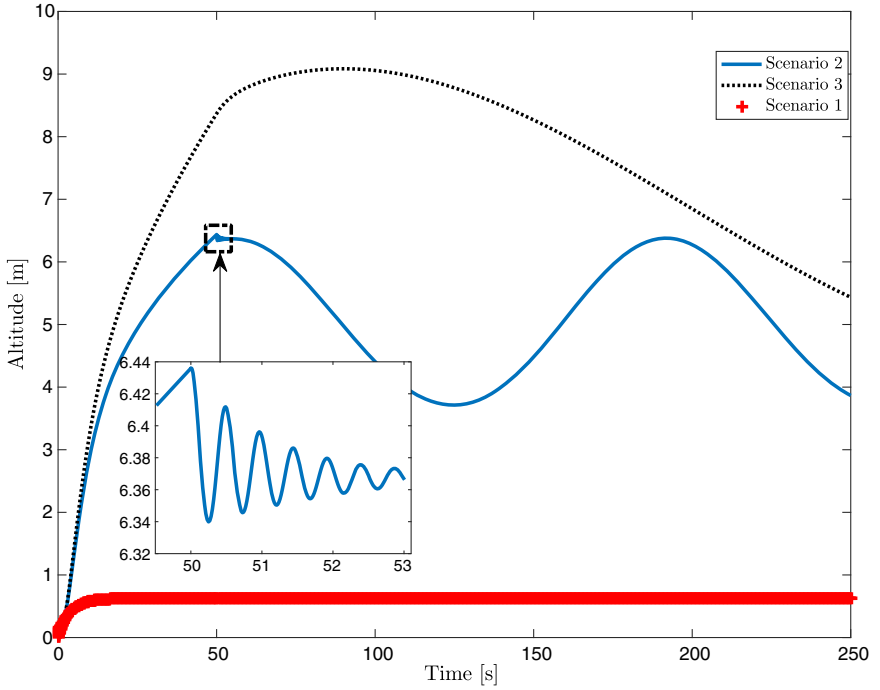

Fig. 3 Altitude of the quadrotor for the three mission scenarios considered.

Figure 3 shows the quadrotor's altitude (that is, $[0, 0, 1]r_{\mathrm{A}}^{\mathbb{I}}(t)$, $t \geq 0$) for the three mission scenarios considered in this example. The aircraft position $r_{\mathrm{A}}^{\mathbb{I}}(t)$, $t \geq 0$, is computed by integrating both the kinematic equations [Eqs. (1) and (2)] and the dynamic equations [Eqs. (8) and (11)]. In all mission scenarios, the quadrotor takes off at $t = 0$. In the first mission scenario, the proportional-derivative control law guarantees that the aircraft hovers at its reference altitude of 0.6 m. In the second mission scenario, the reservoir is connected to the tip of one of the quadrotor's arms, $l = 0.5$ m, $k = 1$ s^{-2}, the exhaust velocity of the reservoir's content is $u_{\mathrm{exhaust},1} = 0.5$ m/s, and the reservoir is dropped at $t_2 = 50$ s; in this case, the quadrotor's altitude varies rapidly at $t = t_2$ and, using the proportional-derivative control law designed for the first mission scenario, its altitude oscillates over time. Specifically, in the short period, the quadrotor experiences high-frequency oscillations of small amplitude, whereas in the long period, the quadrotor experiences low-frequency oscillations of large amplitude. In the third mission scenario, the exhaust velocity of the reservoir's content is $u_{\mathrm{exhaust},2} = 1$ m/s; in this case, the plot of the quadrotor's altitude has a corner at $t = t_2$ and the proportional-derivative control law designed for the first scenario is not able to stabilize the vehicle's altitude.

VI. Conclusions

In this engineering Note is presented, in a tutorial manner, the equations of motion of rotary-wing UASs, for which the inertial properties are not constant functions of time. The current framework allows modeling problems, wherein the UAS mass and moment of inertia vary because of fuel consumption and payloads that are not rigidly connected to the UAS frame. Moreover, this model allows accounting for uncertainties in the location of the vehicle's center of mass.

The unforced translational and rotational dynamic equations involve polynomial nonlinearities only, and hence facilitate the design of computationally efficient control laws. The proposed dynamical model allows accounting for uncertainties in the location of the UAS center of mass by centering the reference frame fixed with the UAS at a conveniently chosen reference point. However, in this case, the UAS translational and rotational dynamic equations are coupled. To reduce the computational load for integrating the coupled set of translational and rotational dynamic equations, disturbance decoupling techniques based on a differential geometric approach can be applied.

In the second part of this Note, the framework is specialized to tackle problems, wherein the UAS mass is constant, the propellers are modeled as thin spinning disks, and the UAS frame is a rigid body. In this case, the equations of motion of rotary-wing UAS commonly available in the literature are deduced. The theoretical framework developed as part of this research is illustrated by a numerical example.

Acknowledgments

This work was supported in part by National Oceanic and Atmospheric Administration (NOAA)/Office of Oceanic and Atmospheric Research under the NOAA–University of Oklahoma Cooperative Agreement no. NA16OAR4320115: the U.S. Department of Commerce.

References

[1] Nonami, K., Kendoul, F., Suzuki, S., Wang, W., and Nakazawa, D., *Autonomous Flying Robots: Unmanned Aerial Vehicles and Micro Aerial Vehicles*, Springer, Tokyo, 2010, pp. 2–24. doi:10.1007/978-4-431-53856-1

[2] Carrillo, L. R. G., López, A. E. D., Lozano, R., and Pégard, C., *Quad Rotorcraft Control: Vision-Based Hovering and Navigation*, Springer, London, 2012. doi:10.1007/978-1-4471-4399-4

[3] Valavanis, K., and Vachtsevanos, G., *Handbook of Unmanned Aerial Vehicles*, Springer, Amsterdam, 2015, pp. 3–12.

[4] Gundlach, J., *Civil and Commercial Unmanned Aircraft Systems*, AIAA, Reston, VA, 2016, pp. 5–11. doi:10.2514/4.103544

[5] Mellinger, D., Michael, N., Shomin, M., and Kumar, V., "Recent Advances in Quadrotor Capabilities," *International Conference on Robotics and Automation*, IEEE Publ., Piscataway, NJ, 2011, pp. 2964–2965. doi:10.1109/ICRA.2011.5980163

[6] Lindsey, Q., Mellinger, D., and Kumar, V., "Construction with Quadrotor Teams," *Autonomous Robots*, Vol. 33, No. 3, 2012, pp. 323–336. doi:10.1007/s10514-012-9305-0

[7] Khalifa, A., Fanni, M., Ramadan, A., and Abo-Ismail, A., "Controller Design of a New Quadrotor Manipulation System Based on Robust Internal-Loop Compensator," *International Conference on Autonomous Robot Systems and Competitions*, IEEE Publ., Piscataway, NJ, 2015, pp. 97–102. doi:10.1109/ICARSC.2015.11

[8] Srikanth, M., Soto, A., Annaswamy, A., Lavretsky, E., and Slotine, J.-J., "Controlled Manipulation with Multiple Quadrotors," *AIAA Guidance, Navigation, and Control Conference*, AIAA Paper 2011-6547, 2011, pp. 1–16.
doi:10.2514/6.2011-6547

[9] Pounds, P. E. I., Bersak, D. R., and Dollar, A. M., "Stability of Small-Scale UAV Helicopters and Quadrotors with Added Payload Mass Under PID Control," *Autonomous Robots*, Vol. 33, No. 1, 2012, pp. 129–142.
doi:10.1007/s10514-012-9280-5

[10] Foehn, P., Falanga, D., Kuppuswamy, N., Tedrake, R., and Scaramuzza, D., "Fast Trajectory Optimization for Agile Quadrotor Maneuvers with a Cable-Suspended Payload," *Robotics: Science and Systems*, Paper 31, 2017, pp. 1–10, http://www.roboticsconference.org/program/papers/31/.

[11] "EnergyOr Shows Off World's First Fuel Cell Multirotor UAV," *Fuel Cells Bulletin*, Vol. 2015, No. 4, 2015, pp. 5–0.

[12] Colgren, R. D., *Applications of Robust Control to Nonlinear Systems*, AIAA, Reston, VA, 2004, pp. 17–40.
doi:10.2514/4.866722

[13] Bouabdallah, S., Noth, A., and Siegwart, R., "PID vs LQ Control Techniques Applied to an Indoor Micro Quadrotor," *International Conference on Intelligent Robots and Systems*, Vol. 3, Sept. 2004, pp. 2451–2456.
doi:10.1109/IROS.2004.1389776

[14] Lanzon, A., Freddi, A., and Longhi, S., "Flight Control of a Quadrotor Vehicle Subsequent to a Rotor Failure," *Journal of Guidance, Control, and Dynamics*, Vol. 37, No. 2, 2014, pp. 580–591.
doi:10.2514/1.59869

[15] Grande, R. C., Chowdhary, G., and How, J. P., "Experimental Validation of Bayesian Nonparametric Adaptive Control Using Gaussian Processes," *Journal of Aerospace Information Systems*, Vol. 11, No. 9, 2014, pp. 565–578.
doi:10.2514/1.I010190

[16] Whitehead, B., and Bieniawski, S., "Model Reference Adaptive Control of a Quadrotor UAV," *AIAA Guidance, Navigation, and Control Conference*, AIAA Paper 2010-8148, 2010, pp. 1–13.
doi:10.2514/6.2010-8148

[17] Besnard, L., Shtessel, Y. B., and Landrum, B., "Quadrotor Vehicle Control via Sliding Mode Controller Driven by Sliding Mode Disturbance Observer," *Journal of the Franklin Institute*, Vol. 349, No. 2, 2012, pp. 658–684.
doi:10.1016/j.jfranklin.2011.06.031

[18] Retha, E. A. A., *Novel Concepts in Multi-Rotor VTOL UAV Dynamics and Stability*, Wiley, New York, 2017, pp. 667–694.
doi:10.1002/9781118928691.ch20

[19] Hoffmann, G., Huang, H., Waslander, S., and Tomlin, C., "Quadrotor Helicopter Flight Dynamics and Control: Theory and Experiment," *Guidance, Navigation and Control Conference*, AIAA Paper 2007-6461, 2007, pp. 2964–2965.
doi:10.2514/6.2007-6461

[20] Bibik, P., Narkiewicz, J., Zasuwa, M., and Żugaj, M., *Quadrotor Dynamics and Control for Precise Handling*, Springer, London, 2016, pp. 335–351.
doi:10.1007/978-3-319-21118-3_19

[21] Müllhaupt, P., "Analysis and Control of Underactuated Mechanical Nonminimum-Phase Systems," Ph.D. Thesis, École Polytechnique Fédérale de Lausanne, Lausanne, Switzerland, 1999.

[22] Kincaid, D. R., and Cheney, E. W., *Numerical Analysis: Mathematics of Scientific Computing*, American Mathematical Soc., Philadelphia, PA, 2002, pp. 109–128.

[23] L'Afflitto, A., *A Mathematical Perspective on Flight Dynamics and Control*, Springer, London, 2017.
doi:10.1007/978-3-319-47467-0

[24] Greenwood, T. D., *Advanced Dynamics*, Cambridge Univ. Press, New York, 2003, p. 1.

[25] Raol, J. R., and Gopal, A. K., *Mobile Intelligent Autonomous Systems*, CRC Press, Danvers, MA, 2016, pp. 511–524.